

AUTOMATIC DETECTION METHOD OF CORONAL MASS EJECTION BY DIGITAL IMAGE ANALYSIS

Nivaor Rodolfo Rigozo

Recebido em 10 setembro, 2010 / Aceito em 8 maio, 2012
Received on September 10, 2010 / Accepted on May 8, 2012

ABSTRACT. This paper intends to present and validate a new automated methodology to detect coronal mass ejections (CME) and determine its dynamics, using digital image processing. This methodology allows determining the CME radial and lateral expansion dynamics. The CME dynamics is determined by selecting a radial direction in a given LASCO image, which starts just before the occulter and extends to the extremity of the image. By taking a series of images, extracting the same radial direction from them and placing them side by side, it is possible to obtain a time history of any moving feature along this direction. This technique allows to choose the number of directions that will be used in CMEs detecting, i.e., in determining their dynamics.

Keywords: coronal mass ejection, CME dynamics, digital image processing.

RESUMO. O objetivo deste trabalho é apresentar e validar uma nova metodologia para detectar automaticamente as ejeções de massas coronais (EMCs) e determinar a sua dinâmica, usando o processamento digital de imagens. Esta metodologia permite determinar a dinâmica radial e de expansão lateral das EMCs. A dinâmica das EMCs é determinada pela seleção de uma direção radial nas imagens do telescópio LASCO, iniciando no centro do ocultador (*occulter*) e estendendo-se até a extremidade da imagem. Se tomarmos uma série de imagens e extrairmos delas a mesma direção radial é possível obter a história temporal de qualquer característica em movimento ao longo desta direção. Esta técnica permite escolher o número de direções que se pode usar na detecção das EMCs, ou seja, na determinação de suas características dinâmicas.

Palavras-chave: ejeções de massas coronais, dinâmica das EMCs, processamento digital de imagens.

INTRODUCTION

CME are solar plasma explosions from the Sun's gravitational field observed in the corona (Hundhausen et al., 1984; Schwenn, 1996; Hundhausen, 1997). These observations are made by instruments called coronagraphs that register the photospheric radiation (or White Light) spread by electrons in the coronal ionized plasma (Brueckner et al., 1995). By following a timeline sequence of these observations is possible to identify these coronal outflows. One of the coronagraphs in operation is the experiment Large Angle and Spectroscopic Coronagraph (LASCO) located in the satellite Solar and Heliospheric Observatory (SOHO) that is a joint project carried by the National Aeronautics and Space Administration (NASA) and the European Space Agency (ESA). LASCO tracks the solar coronal dynamics and observations are made by two coronagraphs called C2 and C3 through corona images from 2-6 and 4-32 solar rays, respectively. When a CME occurs towards the satellite sight line (Sun-Earth path), it appears as a halo structure expanding to all directions, and this is called "CME halo" (Howard et al., 1982).

One of the difficulties faced by the scientific communities is to quantify the observations provided by LASCO images. As a result, techniques were developed to study LASCO images, such as the ones presented by Sheeley et al. (1999) and by Dal Lago et al. (2003a, 2004) to determine CME dynamics. These authors report events with acceleration and deceleration. The acceleration process is closely related to CME formation, while the deceleration is probably related to the CME interaction with the environment ahead, therefore is very important to find out at what distance from the Sun, these processes occur (Dal Lago et al., 2004).

The purpose of this article is to present and validate a new automatic methodology to detect the CME and determine its dynamics (radial and lateral expansion) through digital image processing. To demonstrate its efficiency, the technique was applied in four CME events – on September 28, 1997, February 2, 2001, March 1, 2002 and December 2, 2003 – to quantify these images. This technique presents some similarity to those presented by Sheeley et al. (1999) and Dal Lago et al. (2003a, 2004), however, some fundamental differences do exist: 1 – The new CME dynamics detection method is automatic, while the technique presented by Sheeley et al. (1999) and Dal Lago et al. (2003a, 2004) is done manually. 2 – Another great advantage of this technique, in relation to the other ones, is that it determines the lateral expansion dynamics. As a function of this, determination of CME dynamics is carried out for all directions where the CME events present lateral expansion.

METHODOLOGY

A new Digital Image Processing technique was created based on those aspects presented by Sheeley et al. (1999) and Dal Lago et al. (2003a, 2004). However, a few differences still exist between them. The technique presented by Sheeley et al. (1999) consists of selecting one rectangular radial slice in one given LASCO image, that begins just before the occulter disk and extends to the image extremity. By taking a series of images and extracting the same rectangle (same position) for each one of them and placing them side by side, it is possible to have a timeline history of any characteristic that have dislocated in the interior of such rectangle. These authors utilize the subtraction of images for their analysis, meaning that each image was subtracted from the previous one. Additionally, some corrections of radial intensity were applied, in order to make visible the characteristics at great Sun's distances. Please refer to Sheeley et al. (1999) article to find more details about the referred technique.

Dal Lago et al. (2003a, 2004) technique consists of dividing each LASCO image in angular sectors, not rectangular. Each sector begins in the center of the image, with an aperture angle of 5 degrees. In this way, the area covered by each one of these slices is widened with the solar rays. In this sequence, concentric circles, centered in the center of the image, were placed in the same figure, each one of them with a ray 2 pixels bigger than the other. The slices intersection with the circles, define small areas, and their sizes get bigger with the radial distance from the center. Adding all the pixel values within an area, is the equivalent to accomplish one angular integration. "If in a sequence of images, of the same kind, same spatial resolution, were selected the same "pieces" or "parts" and the same parts are displayed side by side, one would have the dynamic characteristic of the phenomenon within the observed region". This allows to produce one height-time diagram for each angular position and obtain a height-time dispersion graphic.

The technique employed in this work, consists of dividing each LASCO image in punctual angular directions, and not in rectangular or angular sector, each direction begins in the center of the image. The angular distance between two directions (or angular aperture) is defined by us. This is a great advantage over the other methods, once it permits me to control the angular resolution between the directions.

If we take a sequence of images and select the same point for each one of them, and put them side by side, one has a timeline history of the characteristics that dislocate inside this point. In this way it is possible to produce one height-time diagram for each angular position and obtain one graphic of height-time dispersion. This process is illustrated in Figure 1.

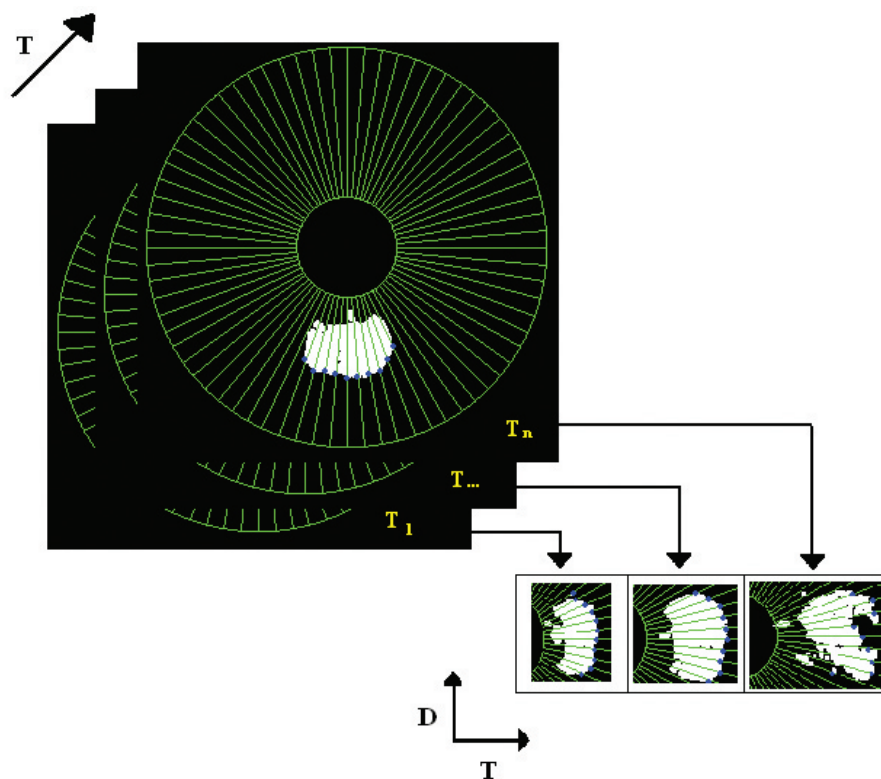


Figure 1 – Illustration of the technique used for image analysis.

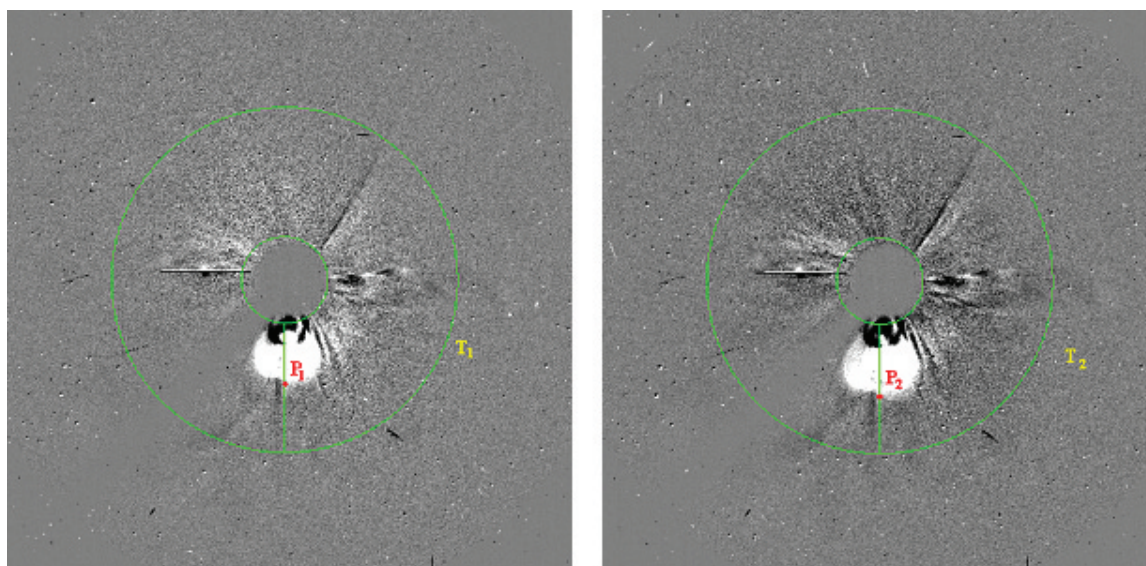


Figure 2 – CME radial position in the T1 and T2 times.

Figure 2 illustrates one example of CME punctual evolution, along the time, for the 180° angular direction. By subtracting the positions P_2 from P_1 , the radial distance (D) traveled by CME in this direction is determined.

Figure 3 shows the positions occupied by CME, in the 180° direction, in time. The time (T) is obtained from the CME image acquisition through LASCO C3. Therefore, the determination of the traveled distance and spent time permits to determine the CME

radial velocity (V) for the 180° angle.

The first (pre-event) image is utilized as a reference (background), all other images are subtracted by the first image before being analyzed. This permits to visualize, clearly, the occurrence of the CME events in the images.

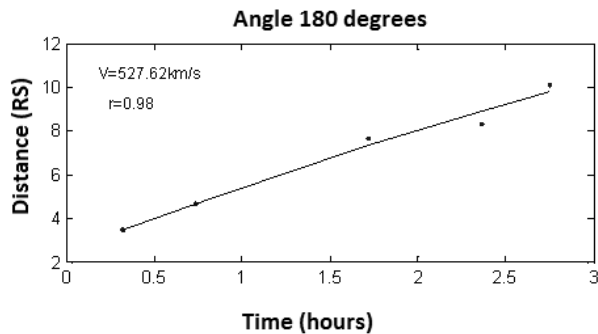


Figure 3 – Position and radial speed of the CME, in time, for the direction of the 180° angle.

RESULTS

In this work four CME events were used, observed by LASCO C3 on September 28, 1997, February 2, 2001, March 1, 2002, and December 2, 2003 (Fig. 4).

Table 1 presents information on images of each CME event observed.

For the September 28, 1997 CME event, eight images were used in the time interval starting at 03:01 (first image) until 09:11 (last image). In the February 2, 2001 CME event, six images were used in the time interval starting at 19:05 (first image) until 23:42 (last image). In the March 1, 2002 CME event, six images were used in the time interval starting at 03:18 (first image) until 06:42 (last image). Finally, in the December 2, 2003 CME event, four images were used, in the time interval starting at 11:18 (first image) until 13:42 (last image), to determine the CME dynamics (Table 1).

Table 1 – Information about the images for each CME observed event.

CME events	Time of 1 st image	Time of last image	Number of images
September 28 – 1997	03:01	09:11	8
February 2 – 2001	19:05	23:42	6
March 1 – 2002	03:18	06:42	7
December 2 – 2003	11:18	13:42	4

For comparison effect with studies done by Dal Lago et al. (2004), only the study of the CME evolution, on September 28, 1997 was carried out for 72 directions, what represents an angular distance of 5 degrees between each direction. The study

of the CME evolution on February 2, 2001 and March 1, 2002 was done for 360 directions, representing an angular distance of 1 degree between each direction, and the study of the CME evolution on December 2, 2003 was completed for 180 directions, representing an angular distance of 2 degrees between each direction. The choice of those different angular resolutions is just to show that the technique allows to choose the angular resolution one wants to work.

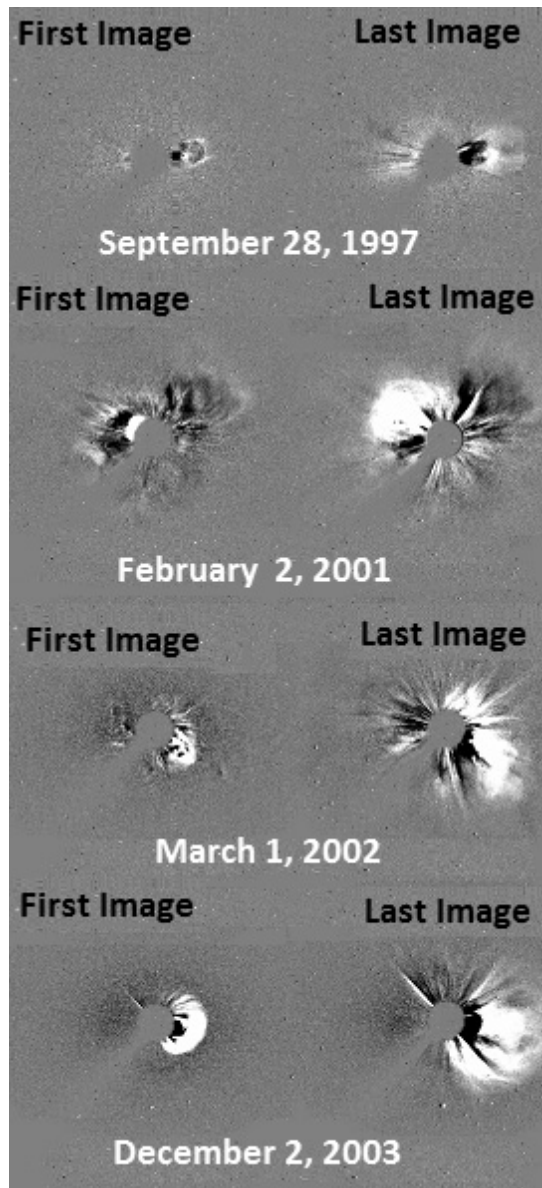


Figure 4 – Four CME events observed by LASCO C3.

Consequently, by applying the new technique to the images of this CME event, one obtains a graph of height dispersion in function of the time (as it is exemplified in Fig. 3) for each one of

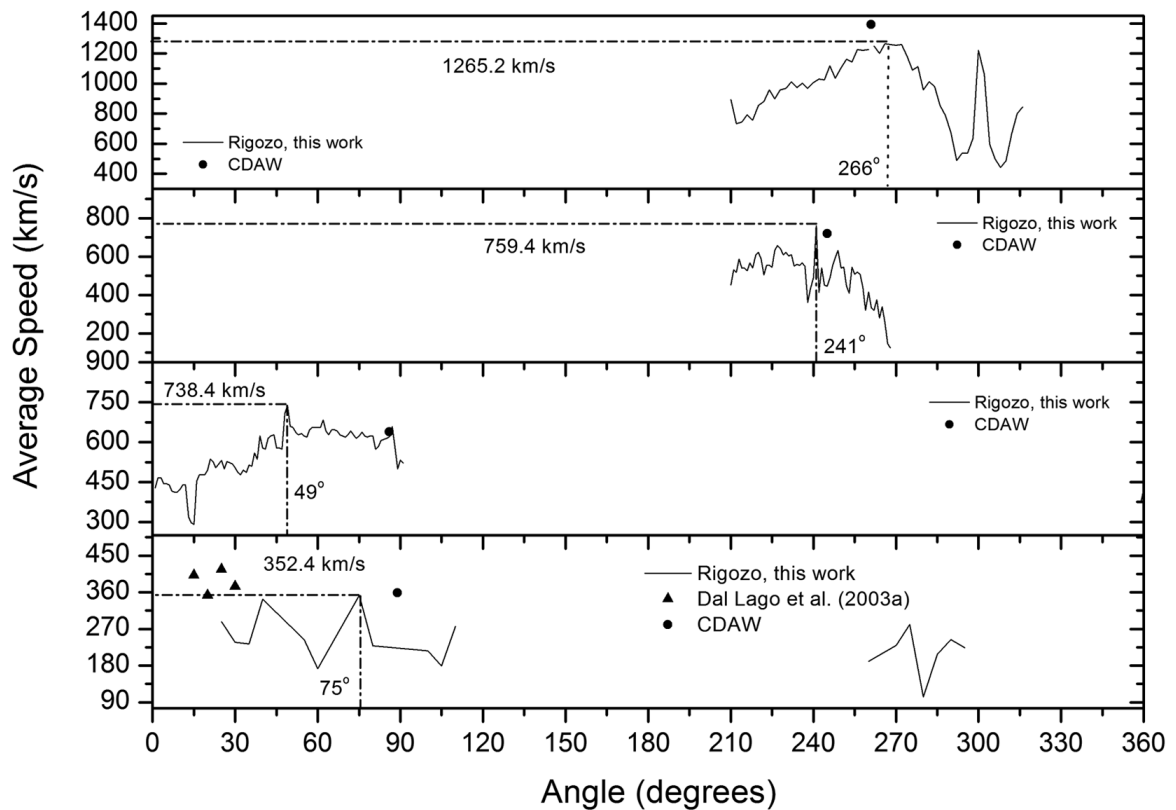


Figure 5 – Radial speed in function of the angle for the CME events on the following days: (A) September 28 (1997), (B) February 2 (2001), (C) March 1 (2002) and (D) December 2 (2003). It is possible to visualize the CME higher speed direction (shown with dotted lines).

the directions, where the “x” axis is the time (hours) and the “y” axis is the radial distance from the center of the Sun (solar rays). The linear adjustment (first order) is used to determine the speed for each position, curve presented in Figure 3. For determining the acceleration, for each position, a second order adjustment is implemented.

The results of the analysis are presented in Figure 5, where the average speeds are plotted as a function of the angle. For the September 28, 1997 event (Fig. 5A), the highest average speed, of 352.4 ± 59.3 km/s, was found for the direction of 75 degrees and it was observed that the CME acceleration was of 10.8 ± 4.3 m/s². In the event of February 2, 2001 (Fig. 5B) the highest average speed of 738.4 ± 93.9 km/s, was found for the direction of 49°, occurring a CME deceleration of -6.3 ± 2.2 m/s. In the March 1, 2002 event (Fig. 5C), the highest average speed of 759.4 ± 121.6 km/s, was found for the direction of 241° and it was observed that occurred a CME deceleration of -28.9 ± 8.5 m/s². Finally, during the December 2, 2003 event (Fig. 5D), the highest average speed of $1,265.2 \pm 234.3$ km/s, was detected for the 266° direction, and there was a CME acceleration of 20.3 ± 9.4 m/s².

DISCUSSION

The height \times time diagrams of the CME events for September 28 (1997), February 2 (2001), March 1 (2002), and December 2 (2003) were obtained using such an image processing technique that allowed us to follow the radial movements of those CME events. The graphs of height dispersion in function of the time, obtained from those diagrams, were well adjusted by a second order polynomial curve, confirming the acceleration and deceleration in those directions.

Dal Lago et al. (2003a) found a radial speed of 416 km/s and an acceleration of 11.6 m/s² for the 25° direction, in the CME event of September 28 (1997). However, the SOHO LASCO CME catalog (CDAW) (http://cdaw.gsfc.nasa.gov/CME_list/) presents a radial speed of 359 km/s and an acceleration of 2.8 m/s² for the 89° direction. While, in this work, it was found a radial speed of 352.4 km/s and an acceleration of 10.8 m/s² for the 75° direction. The average speeds found here were closer to those of the SOHO LASCO CME catalog than the results found by Dal Lago et al. (2003a). The found speed difference was of approximately 2% in relation to the CDAW, while the one from Dal Lago et al.

(2003a) was of 16%. However, the acceleration was an overestimate in relation to the CDAW by the two employed methods. This CME was on the front side and it produced a shock wave in the interplanetary medium, that reached the Earth 71 hours later, on October 1 (1997). On that same day, the ejection that followed such shock wave caused an intense geomagnetic storm that affected the Earth, with a Dst index of -98 nT (Dal Lago et al., 2003a).

CDAW presents a radial speed of 639 km/s and an acceleration of -6.2 m/s² for the 86° direction for the CME event of February 2 (2001). During this work, it was found a radial speed of 738.4 km/s and an acceleration of -6.3 m/s² for the 49° direction. The difference, if compared with the CDAW, was of 15.5% of the average speed and only 1.6% of the acceleration.

In the CME event of March 1 (2002), the CDAW presents a radial speed of 719 km/s and an acceleration of -16.2 m/s² for the 245° direction. During this work it was found a radial speed of 759.4 km/s and an acceleration of -28.9 m/s² for the 241° direction (Fig. 5C). A difference of 5.6% was presented when determining the average speed.

For the CME event of December 2 (2003), the CDAW presents a radial speed of 1,393 km/s and an acceleration of 18.5 m/s² for the 261° direction. While, in this work, it was found a radial speed of 1,265.2 km/s and an acceleration of 20.3 m/s² for the 266° direction (Fig. 5D). If compared with the CDAW data, the average speed difference was of 9.2% and the acceleration difference of 9.7%.

Four CME events were analyzed by this new method, two of them presented an acceleration (September 28, 1997) and December 2, 2003). The CME are driven by the Lorentz force that accelerates the unstable coronal magnetic structure to the speeds that are necessary to be thrown in the interplanetary space (Forbes, 2000). Thus, the CME are ejected and accelerated in the corona's magnetic field and while traveling in the space the magnetic force decreases and other processes can accelerate the CME (Manoharan, 2006). As it is the case of the interaction CME-CME. The effects of the CME-CME interaction can be measured directly when two CMEs are thrown from the same active area. In the case that a second CME goes faster than the first, the result of such interaction is that the first CME will be accelerated while the second will be decelerated (Vršnak et al., 2008).

The other two CME events that were analyzed presented deceleration (February 2, 2001 and March 1, 2002). This happens as a result of the coupling CME-wind, eruptions that are faster than the solar wind, usually decelerate, while those that are slower than the solar wind accelerate (Gopalswamy et al., 2000). Vršnak (2001)

demonstrated that the deceleration is dependent of the speed and height. Fast CME tend to present an accentuated deceleration, where the deceleration decreases with the height, in other words, with the environmental decrease of the density. Such behavior indicates that the CME movements are strongly affected by the aerodynamic dragging, caused by the large-scale emission of MHD waves with wide amplitude, that remove the impulse and energy (Cargill et al., 1996; Cargill, 2004).

Dal Lago et al. (2003b) and Schwenn et al. (2005) proposed the use of the lateral expansion speed of the event of a "CME halo" (as it happened on September 28, 1997), measured in the LASCO C3's images, to predict the CME travel time towards the Earth. The CME lateral expansion speed (VEXP) is defined as the growth rate, approximately, perpendicular to the direction of the radial speed (Dal Lago et al., 2003b; Schwenn et al., 2005) (Fig. 6).

The new technique is able to estimate the speed and acceleration, with a lateral expansion nature, of a CME event, this is an innovation on the methodologies used by Sheeley et al. (1999) and Dal Lago et al. (2003a, 2004). In order to determine the dynamics of CME lateral expansion, the first step is to determine the angular position of the highest radial speed. From this position, the pairs of radial speed are detected, with equidistant angular position (to satisfy the perpendicularity condition, as defined by Dal Lago et al. (2003b) and Schwenn et al. (2005)). The following step is to select the pair that presents the greatest distance among themselves. This distance is indicative of the lateral expansion size (Fig. 7). The temporal evolution of that distance with lateral expansion, which is determined for each LASCO image, represents the CME speed of lateral expansion.

Table 2 – Dynamic characteristics of CME lateral expansion.

V _{exp} (km/s)	a _{exp} (m/s ²)
1,091.3	-0.1
611.7	-0.2
538.8	0.0
1,091.3	-0.1

Table 2 presents information about the speed and lateral expansion acceleration for the CME events. On September 28 (1997), the found expansion speed was of 40.0 km/s. This event did not present an acceleration with lateral expansion. However, on February 2 (2001) the found expansion speed was of 611.7 km/s and presented an expansion deceleration of -0.2 m/s². While on March 1 (2002), the found expansion speed was of 538.8 km/s. This event, also, did not present expansion

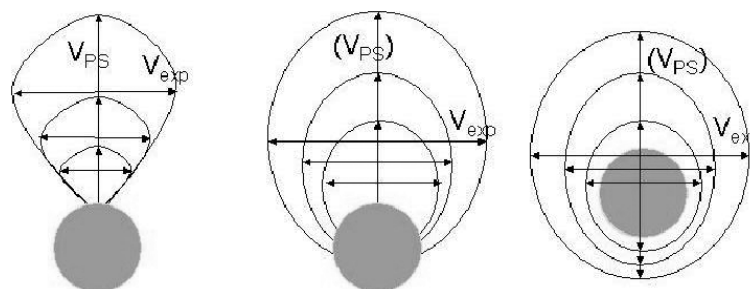


Figure 6 – Illustration of how the expansion speed is defined (V_{exp}) (Schwenn et al., 2005).

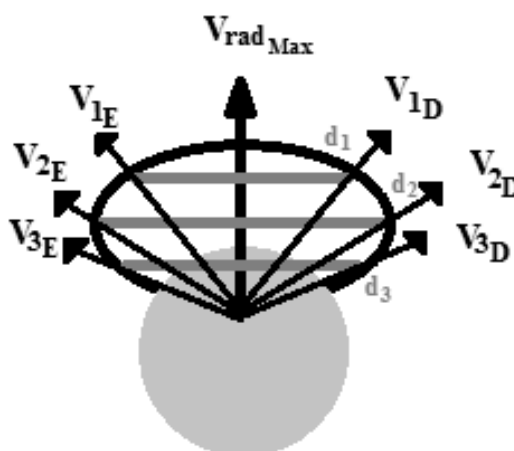


Figure 7 – Illustration of how the method determines the expansion speed (V_{exp}) of a CME event. Where $V_{rad_{max}}$ is the vector of higher radial speed, $V_{1D, 2D, 3D}$ and $V_{1E, 2E, 3E}$ are the pairs of speed vectors (to the left and right of $V_{rad_{max}}$) and $d_{1, 2, 3}$ represent the distances between their respective pairs of speed vectors.

acceleration. Finally, on December 2 (2003), the found expansion speed was of 1,091.3 km/s and presented an expansion deceleration of -0.1 m/s^2 .

This type of measurements can be of extreme importance for the studies of spatial climate, once they can be used to predict the CME travel time towards the Earth (Dal Lago et al., 2004; Schwenn et al., 2005).

The results obtained with the technique for analysis proposed herein, can be considered excellent, once the image data represent phenomena that are millions of kilometers distant from the Earth, and each pixel of the image represents about 39,340 kilometers.

CONCLUSION

This article presented a new methodology to automatically detect the coronal mass ejections (CME) and determine its dynamics, using digital image processing. In order to validate the results obtained by this new and original methodology, it was applied for four CME events: on September 28, 1997, February 2, 2001,

March 1, 2002 and December 2, 2003, and their results were compared with the SOHO LASCO CME catalog (CDAW), and Dal Lago et al. (2003a). The results obtained when validating were good, showing that this methodology is adequate for the study of CME dynamics through digital images.

The advantages of the new methodology in relation to the techniques applied by Dal Lago et al. (2003a) and by the CDAW are: 1) It automatically detects the CME events; 2) It allows to determine the CME dynamics of lateral expansion.

ACKNOWLEDGMENTS

The author gratefully acknowledges the LASCO and teams for permitting the use of the images in this work. Also thankful to the Conselho Nacional de Desenvolvimento Científico e Tecnológico (CNPq) for the financial support in the accomplishment of this work, through the projects: APQ 470252/2009-0 and 301033/2009-9.

REFERENCES

- BRUECKNER GE, HOWARD RA, KOOMEN MJ, KORENDYKE CM, MICHELS DJ, MOSES JD, SOCKER DG, DERE KP, LAMY PL, LLEBARIA A, BOUT MV, SIMNETT GM, BEDFORD DK & EYLES CJ. 1995. The Large Angle Spectroscopic Coronagraph (LASCO). *Solar Phys.*, 162: 357–402.
- CARGILL PJ. 2004. On the Aerodynamic Drag Force Acting on Interplanetary Coronal Mass Ejections. *Sol. Phys.*, 221: 135–149.
- CARGILL PJ, CHEN J, SPICER DS & ZALESK ST. 1996. Magnetohydrodynamic simulations of the motion of magnetic flux tubes through a magnetized plasma. *J. Geophys. Res.*, 101: 4855–4870.
- DAL LAGO A, SCHWENN R, STENBORG G & GONZALEZ WD. 2003a. Coronal mass ejection speeds measured in the solar corona using LASCO C2 and C3 images. *Adv. Space Res.*, 32(12): 2619–2624.
- DAL LAGO A, SCHWENN R & GONZALEZ WD. 2003b. Relation between the radial speed and the expansion speed of coronal mass ejections. *Adv. Space Res.*, 32(12): 2637–2640.
- DAL LAGO A, SCHWENN R, STENBORG G, GONZALEZ WD, GONZALEZ ALC, VIEIRA LEA, ETHER E, GUARNIERI FL & SCHUCH NJ. 2004. Deceleration observed on the July 25 (1999) coronal mass ejection. *Geofisica International*, 439(1): 41–45.
- FORBES TG. 2000. A review on the genesis of coronal mass ejections. *J. Geophys. Res.*, 105: 23153–23166.
- GOPALSWAMY N, LARA A, LEPPING RP, KAISER ML, BERDICHEVSKY D & ST CYR OC. 2000. Interplanetary acceleration of coronal mass ejections. *Geophys. Res. Lett.*, 27: 145–148.
- HOWARD RA, MICHELS DJ, SHEELEY NR Jr & KOOMEN MJ. 1982. The observation of a coronal transient directed at Earth. *Astrophys. J.*, 263: 101–104.
- HUNDHAUSEN AJ. 1997. An introduction. In: CROOKER N, JOSELYN JA & FEYNMAN J. (Eds.). *Coronal mass ejections*. Washington, DC: AGU, 99: 1–7.
- HUNDHAUSEN AJ, SAWYER CB, HOUSE LL, ILLING RME & WAGNER WJ. 1984. Coronal mass ejections observed during the solar maximum mission – latitude distribution and rate of occurrence. *J. Geophys. Res.*, 89: 26–39.
- MANOHARAN PK. 2006. Evolution of Coronal Mass Ejections in the Inner Heliosphere: A Study Using White-Light and Scintillation Images. *Sol. Phys.*, 235: 345–368.
- SCHWENN R. 1996. An essay on terminology, myths, and known facts: solar transients – flare – CME – driver gas – piston – BDE – magnetic cloud – shock wave – geomagnetic storm. *Astrophys. J.*, 243: 187.
- SCHWENN R, DAL LAGO A, HUTTUNEN E & GONZALEZ WD. 2005. The association of coronal mass ejections with their effects near the Earth. *Annales Geophysicae*, 23: 1033–1059.
- SHEELEY Jr NR, WALTERS JH, WANG Y-M & HOWARD RA. 1999. Continuous tracking of coronal outflows: two kinds of coronal mass ejections. *J. Geophys. Res.*, 104(A11): 24739–24767.
- VRŠNAK B. 2001. Deceleration of Coronal Mass Ejections. *Sol. Phys.*, 202: 173–189.
- VRŠNAK B, VRBANEC D & CALOGOVIĆ J. 2008. Dynamics of coronal mass ejections – The mass-scaling of the aerodynamic drag. *Astronomy & Astrophysics*, 490: 811–815.

NOTES ABOUT THE AUTHOR

Nivaor Rodolfo Rigozo. Doctor in Space Geophysics, INPE – Instituto Nacional de Pesquisas Espaciais (1998), currently researcher at Centro Regional Sul de Pesquisas Espaciais, an INPE division in the Rio Grande do Sul State. Nowadays studying the Sun-Earth relationship through Natural Registers by the analysis of temporal series, and analysis of digital images of coronal mass ejections (CME) events.